



0008-8846(94) 00042-5

OPTIMIZATION OF ULTRA-HIGH-PERFORMANCE CONCRETE BY THE USE OF A PACKING MODEL

F. de Larrard and T. Sedran
Laboratoire Central des Ponts et Chaussées
PARIS - France.

(Communicated by M. Moranville-Regourd)

(Received September 23, 1993)

ABSTRACT

The concept of high packing density has been recently rediscovered, as a key for obtaining ultra-high-performance cementitious materials. First, this paper presents two models allowing to predict the packing density of a particle mix. These models are derived from the Mooney's suspension viscosity model. At a second step, considerations on the parameter to be maximized during the mix-design process are presented. Reference is made to the Maximum Paste Thickness concept, which leads to choose a fine sand for optimizing the compressive strength of cementitious materials. Then, an optimal material is sought, based on the following requirements: fluid consistency, classical components (i.e. ordinary aggregate, sand, Portland cement, silica fume, superplasticizer, water), and moderate thermal curing. A selection of mixes is made with the help of the Solid Suspension Model, and tests are performed in order to verify that the mix obtained is definitely optimal. The final result is the production of a fluid mortar having a water/binder ratio of 0.14 and a compressive strength of 236 MPa.

KEYWORDS

High-strength concrete, mathematical model, packing density, silica fume, superplasticizer, viscosity.

INTRODUCTION

Thanks to superplasticizers and silica fume, it has been possible to produce in laboratory concrete with a cylinder compressive strength of about 150 MPa [1]. On site, the maximum achieved value seems to be 115-120 MPa at 28 days (in Two Union Square building, Seattle). Such high-performance material can be of interest not only for the mechanical strength, but also for some other aspects, like higher modulus, lower creep and shrinkage, or better durability [2].

Much higher strengths have been obtained in the laboratory by using special techniques such as autoclaving, compaction under high pressure, or impregnation with polymers [3, 4]. However, this kind of techniques requires expensive facilities, and is sometimes difficult to apply to full-size elements like beams or slabs. For instance, efficient autoclaving entails penetration of water vapour in the concrete porosity, a difficult goal to match when the concrete piece thickness is higher than a few centimetres. On the other hand, materials incorporating special polymers (like Macro-Defect Free cements, MDF) may display some drawbacks like a high sensitivity to water [5]. Another way of increasing compressive strength is the use of special aggregates [6, 7] like calcined bauxite. Bache [6] reported on a high-grade DSP mortar having a compressive strength of 268 MPa. But these aggregates are expensive, so that their industrial interest is limited.

Therefore, the research significance of the present paper is to see which strength level can be presently obtained by using normal untreated aggregates, cement, silica fume and superplasticizer, when a simple thermal curing is available (comprising only a temperature rise, but neither additional pressure nor humidity). This kind of curing is expected to be feasible as well on site as in ordinary precasting plant. Optimisation is carried out with the help of a mathematical model, together with preliminary testing, in order to reduce the number of tests and to propose a general mix-design methodology. The model deals with the material at the fresh state. Here, the problem is to find the proportion leading to the best packing density of particles [6, 3].

MODELLING THE PACKING DENSITY OF GRAIN MIXTURES

The Linear Packing Density Model for grain mixtures (LPDM)

In 1951, Mooney developed a model for predicting the viscosity of multimodal suspensions of non-reactive particles [8]. We have shown that this model can be used as a packing model, just by searching the liquid proportion leading to infinite viscosity [9]. A large number of dry packing experiments have allowed a calibration of this packing model, either for crushed or rounded particles [10]. Equations of the Linear Packing Density Model (LPDM) are the following:

$$c = \min(c(t)) \text{ for } y(t) > 0 \text{ with} \tag{1}$$

$$c(t) = \frac{\alpha(t)}{1 - \int_d^t y(x)f(x/t)dx - [1 - \alpha(t)] \int_t^D y(x)g(t/x)dx} \tag{2}$$

$$f(z) = 0.7(1 - z) + 0.3(1 - z)^{12} \tag{3}$$

$$g(z) = (1 - z)^{1.3} \tag{4}$$

where c is the packing density, t the size of the grains, $y(t)$ the voluminal size distribution of the grain mixture (having a unit integral: $\int_d^D y(x)dx = 1$); d and D are respectively the minimum and

maximum sizes of grains, $\alpha(t)$ is the specific packing density of the t -class, $f(z)$ is the *loosening effect* function and $g(z)$ is the *wall effect* function. These functions, describing the binary interactions between size classes, are expected to be universal, while $y(t)$ and $\alpha(t)$ depend on the considered granular mix, and can be measured.

LPDM has shown good performances in predicting optimal proportions of superplasticized cementitious materials (cement pastes [11], mortars and concretes [10]). But it suffered from an original defect, owing to its linear nature: curves giving relationship between packing density and proportions exhibit angular points in the vicinity of optimal values. Such a feature does not appear in practice (see fig. 1). This is why a better model is needed.

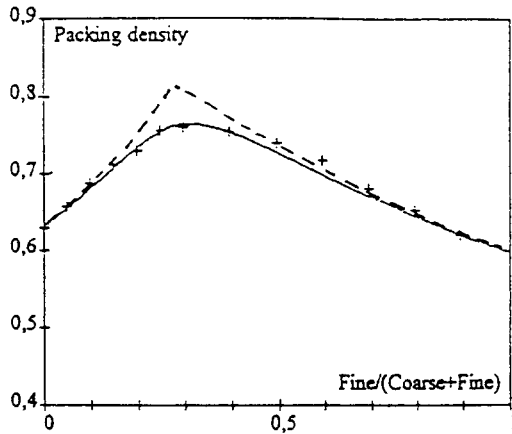


FIG. 1: Packing density versus fine grains content (binary mix of rounded aggregates of 0.5 and 8 mm diameter). Solid line: LPDM; dotted line: SSM; crosses: experimental values.

A new packing model: the Solid Suspension Model (SSM)

In this last development, we have come back to Mooney's original model, by considering a random packing of particles like a suspension of high, but finite viscosity. Therefore, the reference specific packing densities are shifted towards higher values. For example, it is well known that a monodisperse arrangement of spheres may achieve a packing density of 0.74 (compact hexagonal arrangement), while a random packing of the same particles gives no more than 0.64 [12]. Following Mooney's model, the relationship between the solid content of a monodisperse suspension ϕ and its relative viscosity η_r is:

$$\eta_r = \exp\left(\frac{2.5}{1/\phi - 1/\beta}\right) \tag{5}$$

Here, we will assume that β represents the maximum packing density, while ϕ is the random one. With $\beta = 0.74$ and $\phi = 0.64$, one have $\eta_r = 1.36 \cdot 10^5 = \eta_r^{ref}$.

Then, with the same formalism as in LPDM, the packing density for any grain mixture is given in the following implicit equation:

$$\eta_r^{ref} = \exp\left[\int_d^D \frac{2.5y(t)}{1/c - 1/c(t)} dt\right] \text{ with} \tag{6}$$

$$c(t) = \frac{\beta(t)}{1 - \int_d^t y(x)f(x/t)dx - [1 - \beta(t)] \int_t^D y(x)g(t/x)dx} \tag{7}$$

where $\beta(t)$ is the *virtual* specific packing density of t-size grains calculated from $\alpha(t)$ the *experimental* (random arrangement) one with the next equation

$$\eta_r^{ref} = \exp\left(\frac{2.5}{1/\alpha(t) - 1/\beta(t)}\right), \text{ for } d \leq t \leq D. \tag{8}$$

When a t-size class consists of N different types of grains, each one characterized for $i=1$ to N, by its own partial volume $y_i(t)$ (with $\sum_{i=1}^N y_i(t) = 1$) and $\beta_i(t)$, the overall virtual packing density $\beta(t)$ is

$$\text{defined by: } \frac{1}{\beta(t)} = \sum_{i=1}^N \frac{y_i(t)}{\beta_i(t)} \tag{9}$$

In fact, as they have the same size, the different types of grains are supposed to have no influence on the packing of the other ones. According to that, the solid volume $y_i(t)$ occupies the volume $\frac{y_i(t)}{\beta_i(t)}$. Then, the solid volume $\sum_{i=1}^N y_i(t) = 1$ is contained in the total volume $\sum_{i=1}^N \frac{y_i(t)}{\beta_i(t)}$ which justifies the expression of $\beta(t)$.

Figure 1 highlights the decisive improvement of the original model allowed by SSM. Note that SSM can also be used to predict the solid content of a suspension of a given viscosity η_r just by replacing in equation (6) η_r^{ref} by this new viscosity.

FERET'S GENERALIZED FORMULA FOR COMPRESSIVE STRENGTH - EFFECT OF MAXIMUM PASTE THICKNESS

One hundred years ago, Féret proposed what seems to be the first formula for predicting the compressive strength of cementitious material [13]. The fact that it is mainly the *nature* of cement paste that governs the concrete strength underlies this well-known expression. At a first step, we have proposed a generalised form of Féret's equation, in order to take the role of silica fume into account [14, 15]. This formula is not expected to apply to the present research, because it deals with normally cured mortars and concretes. However, Féret's formulas show that the maximum strength is attained when the matrix initial porosity (MIP)[11], i.e. the ratio of voids per total matrix volume, is minimal. This principle will be assumed to remain valid.

The aggregate does also influence the compressive strength of high-strength materials [1]. A first condition is to use an aggregate whose strength is higher than the one of the desired concrete. Recently, we have investigated in more details the variations of concrete compressive strength with the *topology* of the aggregate skeleton [16]. We have shown that, in case of rounded aggregates, the second parameter governing the concrete compressive strength is the *Maximum Paste Thickness* (MPT). This physical parameter represents the mean distance between two coarse aggregates, assuming that each aggregate is surrounded by a paste layer, whose thickness is proportional to the aggregate diameter. The MPT can be evaluated by the following equation:

$$e_M = D(\sqrt[3]{g^*/g} - 1), \quad (10)$$

where e_M is the MPT, D is the maximum size of aggregate, g^* is the packing density of the aggregate (not to be confused with the one of the whole mix) and g is the actual volume of aggregate in the mix.

The compressive strength has been found to decrease when the MPT increases from 0.1 to 5 mm. Thus, the aggregate has a positive *confining effect* on the cement paste. Accounting for this effect in Féret's equation leads to halve the mean error of the predictions, as compared to experimental values. The influence of MPT explains why, when the nature of a concrete matrix is constant, the strength decreases when the paste volume increases [17], or why a small maximum size of aggregates leads to higher strength in some high-strength concretes [16].

IMPLICATIONS FOR OPTIMIZATION OF ULTRA-HIGH-PERFORMANCE MATERIAL

First of all, a reference viscosity should be chosen, depending on the production method. The higher the viscosity, the lower the minimum water content. However, if the mix is too sticky, the entrapped air volume will increase. Therefore, a critical viscosity should be determined, allowing to obtain a minimal content of voids.

Secondly, the minimal matrix porosity should be looked for. This criterion leads to the determination of the silica fume/cement ratio. However, any increment of aggregate volume increases the viscosity, entailing an increase of the *matrix* porosity in order to keep the viscosity constant. This is why this approach would lead to a pure paste [18]. On the other hand, in such a case, the MPT would become infinite ($g = 0$ in equation 10). This is why a certain aggregate content should be adopted, for limiting the second term in equation 10. However it may be, the best material will have a very low overall porosity. Thus a first approach is to test different mixes having such a low porosity to underline the respective influence of each parameter.

For minimising MPT, it is possible to act on the size of aggregate. From this point of view, the minimal D is desirable. On the other hand, as a dense packing of the matrix is aimed at, the d size should be high enough as compared to the maximum size of cement grains, in order to reduce the *wall effect*. Therefore, a monosize sand appears to be the best solution. This is why a ultra-high-performance concrete will be generally a ultra-high-performance mortar.

CHOICE OF COMPONENTS

Cement

The cement used for this project is an ordinary Portland cement. As it can be seen in table 1, this cement contains very few C_3A , which minimises its water demand [14, 19].

Its grading, as measured by a LASER analyser, appears in table 2. The packing density of the cement is determined by measuring the water content of a superplasticized cement paste whose consistency is intermediate between a humid soil and a homogenous paste (see table 4).

TABLE 1. Characteristics of CPA 55 HTS cement from Le Teil

Chemical analysis in %		Potential composition according to Bogue in %	
Soluble silica	22.75	C_3S	67.23
Aluminium Oxide	2.86	C_2S	14.5
Titanium oxide	0.33	C_3A	4.11
Ferric oxide	2.05	C_4AF	6.23
Calcium oxide	67.36	Gypsum	4.21
Magnesium oxide	0.63	$CaCO_3$	1.43
Sodium oxide	0.11	Free lime	0.78
Potassium oxide	0.14		
Sulphuric Anhydride	1.96	Compressive strength on ISO mortar in MPa	
Chlorine of chlorides	0	1 day	16.5
Sulphur of sulphides	0	7 days	32.8
Insoluble residue	0.3	28 days	54.0
Ignition loss	1.04	Flexural strength of an ISO mortar in MPa	
Manganese oxide	0.02	1 day	3.9
Total	99.55	7 days	7.0
Free lime	0.78	28 days	9.5
Carbonic anhydride	0.63		
Density	3150 kg/m ³		

TABLE 2. Gradings of solid components (% passing).

t (μm)	Silica fume	Cement	Sand S125	Sand S250	Sand S400	t (μm)	Silica fume	Cement	Sand S125	Sand S250	Sand S400
0,080	0	0	0	0	0	6.30	98	26	0	0	0
0.100	0	0	0	0	0	8.00	99	32	0	0	0
0.125	18	0	0	0	0	10.0	100	38	0	0	0
0.160	39	0	0	0	0	12.5	100	43	0	0	0
0.200	57	0	0	0	0	16.0	100	52	0	0	0
0.250	76	0	0	0	0	20.0	100	60	0	0	0
0.315	77	0	0	0	0	25.0	100	68	0	0	0
0.400	79	0	0	0	0	31.5	100	78	0	0	0
0.500	81	2	0	0	0	40.0	100	87	0	0	0
0.630	82	3	0	0	0	50.0	100	93	0	0	0
0.800	84	5	0	0	0	63.0	100	95	0	0	0
1.00	86	6	0	0	0	80.0	100	97	13	0	0
1.25	87	6	0	0	0	100	100	100	56	0	0
1.60	89	7	0	0	0	125	100	100	100	2	2
2.00	91	9	0	0	0	160	100	100	100	19	16
2.50	92	11	0	0	0	200	100	100	100	53	43
3.15	94	13	0	0	0	250	100	100	100	100	80
4.00	95	18	0	0	0	315	100	100	100	100	96
5.00	97	22	0	0	0	400	100	100	100	100	100

Aggregate

A quartz sand is used (with 3 different gradings), because of the very high-strength of the original massive rock. Rounded grains are preferred from a rheological point of view. The density of the sands is 2680 kg/m^3 . Gradings of the different sands are summarised in table 2, as determined by sieving. The packing density of each sand is measured by weighing a one litre container filled up with sand consolidated on a vibrating table during two minutes (see table. 4).

Silica fume

A recent study [20] has shown that the pozzolanic activity of a silica fume is reduced by its alkali content; moreover, the fluidity of fresh concrete increases when the carbon content of the silica fume decreases. For these reasons, a white silica fume (a by-product of zircon production) is chosen, whose characteristics are given in table 3.

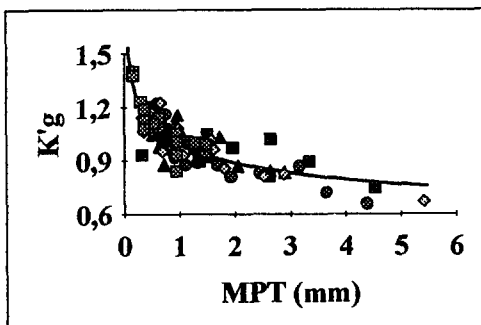


FIG 2. Effect of Maximum Paste Thickness on compressive strength (non-dimensional parameter) [16].

Chemical analysis		BET specific area
SiO ₂	92.7%	14 m ² /g
Na ₂ O	0.71%	
K ₂ O	0.12%	Density
C	0%	2350 kg/m ³

TABLE 3. Characteristics of the 'SEPR' silica fume

As for the other components, the grading of silica fume was needed in order to use the SSM model. The silica fume grading is determined with a Sedigraph in the range of 0.25 to 50 μm. As a great part of the silica particles are smaller than 0.25 μm, assumptions should be made to describe the finest part of the grading. The size distribution is supposed bilinear [14] as shown in figure 3 and according to the following equations:

- $p_1(t) = 0,065 \ln t + 0,85$ for $0,25 < t < 10$ (11)

- $p_2(t) = 0,83 \ln t + 1,91$ for $t_{min} < t < 0,25$ with $t_{min} = 0,1 \mu m$ (12)

The different values of parameters in equations 11 and 12 are calculated by writing the boundary equalities:

- $p_1(10) = 1$ (13)

- $p_1(0,25) = p_2(0,25) = 0,76$ (14)

- $p_2(t_{min}) = 0$ (15)

$$S_{bet} = 6000 \int_{t_{min}}^{10} \frac{dp(x)}{\rho x} \tag{16}$$

where S_{bet} (in m²/g) is the specific surface of the silica fume estimated according to BET procedure and ρ its density (in kg/m³).

The grading obtained for silica fume appears in table 2.

The same method as the one used for cement is adopted to measure the packing density of the silica fume (see table 4).

Superplasticizer

After some tests on slurries with Marsh's cone [18], a melamine superplasticizer ('ChrysoSuperplast') with 40% solid content is selected because it brings an important and durable fluidification of mixes. The saturation quantity (in solid content) is estimated to be 1.3% of the cement content plus 2% of the silica fume content.

EXPERIMENTS

Calibration of SSM

A preliminary mathematical development is necessary prior to the application of SSM: the specific packing density function $\alpha(t)$ must be determined. The size of 1 μm is known to be the upper limit for colloidal particles, so $\alpha(t)$ is assumed to be defined by the following equations:

- $\alpha(t) = p \ln(t) + q$ if $t < 1 \mu m$ (17)

- $\alpha(t) = q$ if $t > 1 \mu m$ (18)

As its particles are spherical, the q value for the silica fume is estimated to be 0,64. Then the p value is fitted in order to find the same packing density with SSM as with experiments (see table 4). The p value for the cement is supposed to be the same as for silica fume and then the p value is fitted. Finally, as all the sands particles are greater than $1 \mu\text{m}$, only the q values are fitted. Thus, packing densities can be predicted by using equations 6, 7 8 and 9, for any set of dry material proportions.

TABLE 4. Packing constants of solid components.

Components	S400	S250	S125	OPC	Silica fume
Experimental packing densities	0,615	0,603	0,599	0,65	0,72
Packing densities as given by SSM	0,616	0,605	0,597	0,647	0,716
Coefficient p of equation 17	/	/	/	0,015	0,015
Coefficient q of equations 17 and 18	0,565	0,565	0,565	0,445	0,64

Batching and Curing

Mortars are prepared with a conventional 3-speed mixer. After some preliminary tests, the mixing procedure is the following:

- mixing of water, silica fume and 33% of superplasticiser till the slurry looks homogenous;
- progressive incorporation of cement with 50 % of superplasticiser;
- incorporation of sand, and mixing for 1 minute at high speed;
- addition of the residual 17% of superplasticiser and mixing for 1 minute at high speed.

For each batch, the air content is measured with an air-meter after a 2-minutes vibration on a vibrating table. For series-I mixes, two cylinders (110x110mm) are cast in mould using the same vibration. The cylinders are demolded after 24 hours then protected with two aluminium sheets in order to avoid any exchange of humidity and stored 72 hours at 20°C. Next, the cylinders are cured at 90°C at the atmospheric pressure during 48 hours. They are then slowly and naturally cooled during 20 hours in an insulating box, in order to avoid a too severe thermal gradient. The cylinders are finally lapped before being tested in compression.

Selection of mixes and test results

The detailed composition of the mixes compositions and their properties are summarised in table. 5. In mixes #1 to 3, the mortar viscosity and the paste composition are kept constant, while the

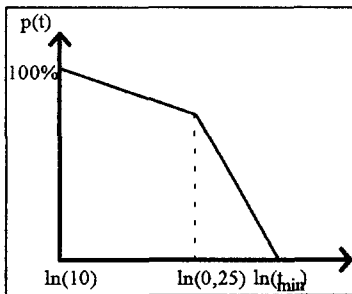


FIG. 3. Assumed grading shape for silica fume

maximum size of aggregate changes. Thus, the MPT ranges from 0.088 to 0.046 mm. Surprisingly, no strength increase is noted when MPT decreases. A first conclusion is that, in this range of very low MPT, the effect of this parameter reaches a maximum level and doesn't have anymore the effect on the compressive strength as predicted in figure 2.

Based on the previous results, the s400 sand is chosen. Then, for a relative viscosity of 10^4 , the mix giving a minimum water demand is chosen (#4). Mixes #5 to 8 have the same powders composition, but contain less water. As expected, this lead to higher viscosities and air contents, and gives lower compressive strength.

Supplementary mixes 9, 10, 11 represent the extreme values of W/(W+S) ratio obtained in the scope of this study. Air content of mixes #9 is quite great high to its higher viscosity. The increase of aggregate volume in mixes #10 and 11 allows high W/(W+S) ratios with few changes in the viscosity.

It's interesting to mention that mixes #4 and 11 have the same overall initial porosity (same air content and same water content) but quite different resistances. Thus, minimising the overall initial porosity doesn't seem to be a sufficient condition to obtain the strongest materials.

Finally it can be noted that some of the mixes proposed in table 5 are quite close to the mortar composition recently patented by Richard et al. [21].

Due to the upper limitation of the MPT effect, it has been decided to test also some pure pastes (mixes #12 to 15). Various silica/cement ratios are used, together with various viscosities. Obtained maximum strength is comparable with the one of the mortars.

Discussion - Effect of matrix final porosity (MFP)

We have emphasized the role of the initial porosity of the matrix in the strength of cementitious material. However, it would be more logical to refer to the porosity of hardened material. Let us assume that, with the help of thermal curing, almost all the water is chemically combined with the cement. Considering that 1 g of cement needs 0,25 g of water to be fully hydrated, and assuming that the *Le Chatelier* contraction during hydration is about 10%, the contribution of water to the final porosity is:

$$0.1(1/3.1 + 0.25)/0.25 = 0.23$$

Thus, the matrix final porosity π_M can be evaluated (see table 6) by the following formula:

$$\pi_M = (0.23 v_w + v_a)/(1 - g) \quad (19)$$

where g , v_w and v_a are respectively the partial volumes of aggregate, water and air.

A rough correlation is found between this parameter and the compressive strength, respectively for the tested mortars (figure 4) and pastes (figure 5). Deviations from a direct relationship between these parameters are attributed to the lack of accuracy in the measurement of air content, and the important dispersion of compressive tests despite the great care taken during tests. At equal MFP, the mortar strength is higher than the paste one, confirming the beneficial confining effect of the aggregate.

Further characterisation of optimal mix

The optimal mortar mix (#4) is more deeply characterized, by a second series of tests. Fifteen 110x220 mm.-cylinders were cast, 12 of which being normally cured in water at 20°C, the last 3 being thermally cured like the previous series, but with a shorter preheating period (2 days) and a longer thermal treatment (4 days). The results of the tests completed are summarized in table 7.

TABLE 5. Composition and properties of the different mixes (series I).

N°	η_r	Sand type	Silica fume (%) *	Cement (%) *	Sand (kg)	Cement (kg)	Silica fume (kg)	Water (kg)	W/C	S/C	W/(C+S)	Air (%)	MPT (mm)	MFP	Rc (MPa)
1	10000	s400	16.0	51.5	724.9	1148.6	356.9	199.6	0.174	0.311	0.133	2.7	0.088	0.100	232.7
2	10000	s250	16.2	52.5	697.4	1167.9	359.3	202.7	0.174	0.308	0.133	2.5	0.079	0.097	229.0
3	10000	s125	18.0	57.9	526.9	1265.8	393.5	220.5	0.174	0.311	0.133	3	0.046	0.100	223.6
4	10000	s400	15.0	48.5	813.2	1080.6	334.2	198.2	0.183	0.309	0.140	2.6	0.075	0.103	237.9
5	20000	s400	15.0	48.5	824.5	1095.6	338.9	187.0	0.171	0.309	0.130	4.6	0.073	0.129	214.5
6	40000	s400	15.0	48.5	834.8	1109.3	343.1	176.9	0.159	0.309	0.122	4.7	0.072	0.127	221.1
7	80000	s400	15.0	48.5	842.9	1120.1	346.4	168.9	0.151	0.309	0.115	5.8	0.071	0.141	229.0
8	100000	s400	15.0	48.5	845.3	1123.3	347.4	166.5	0.148	0.309	0.113	5.7	0.070	0.139	224.0
9	40000	s400	18.0	60.0	502.4	1370.2	411.1	188.6	0.138	0.300	0.106	6	0.138	0.127	222.9
10	18000	s400	12.1	39.0	1088.3	868.0	269.3	191.3	0.220	0.310	0.168	1.9	0.041	0.106	224.0
11	10000	s400	12.1	39.0	1076.0	858.2	266.3	200.5	0.234	0.310	0.178	2.4	0.043	0.117	216.7
12	5000	-	36.0	64.0	0.0	1339.4	753.4	244.0	0.182	0.562	0.117	5.1	∞	0.107	177.2
13	10000	-	25.0	75.0	0.0	1647.1	549.0	231.1	0.140	0.333	0.105	7	∞	0.123	192.9
14	2000	-	20.0	80.0	0.0	1682.8	420.7	274.5	0.163	0.250	0.130	1.6	∞	0.079	244.9
15	500	-	20.0	80.0	0.0	1601.7	400.4	309.5	0.193	0.250	0.155	1.2	∞	0.083	207.8

* Weight percentage of dry powders

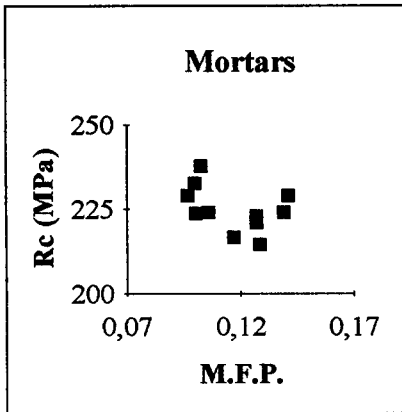


FIG. 4. Strength of mortars vs. Matrix Final Porosity, as predicted by equ.19.

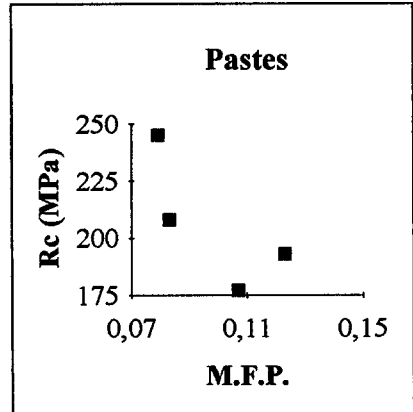


FIG. 5. Strength of mortars vs. Matrix Final Porosity, as predicted by equ.19

TABLE 6. Tests on optimal mix (series II).

Composition (kg/m ³)		Properties	
		With water curing	With thermal curing
Sand	813.2	Compressive strength (MPa)	Compressive strength (MPa)
Cement	1080.6	1 day	7 days
Silica fume	334.2	7 days	235.8
Water	198.2	28 days	
		Tensile splitting strength (MPa)	
Air content	2%	28 days	
Flowing time (Maniabilimètre LCL)	1 second	Young's modulus (GPa)	
		28 days	

As compared to mix #4 in series I, the compressive strength of thermally cured samples is the same, while the slenderness of the samples is higher (see table 6). This is probably due to the longer thermal curing in this series (4 days instead of 2 days). Otherwise, the beneficial effect of thermal curing on the ultimate strength of very low water-cement ratio concretes, already mentioned by Kokkila [7], is verified.

CONCLUSION

The Solid Suspension Model is a valuable tool to optimize high packing density cementitious materials. Using the equipment available for this study, it allowed to produce a fluid mortar with a 0.14 water-binder ratio.

In order to maximize the compressive strength with a set of components, it is first desirable to use only fine sand for aggregate; then a moderate theoretical viscosity is chosen (about 10⁴ the one of water). Finally the Matrix Final Porosity, as predicted by equation 19, is taken very low while keeping an aggregate volume sufficient sufficient enough to confine the paste.

A simple thermal curing (at normal pressure and humidity) is an efficient way to increase the final compressive strength of ultra-low water-binder ratio mortars. Here, a value of 236 MPa has been

achieved with a 4-day curing at 90°C. Thus a new range of 200 MPa-mortars, requiring only a moderate thermal curing, appears to be industrially feasible.

Further research is necessary to determine the critical Maximum Paste Thickness under which the influence of this parameter on compressive strength reaches a maximum. Once this value is known, an economical optimization will be possible. Also, many questions concerning this new type of ultra-high-performance mortars are still open, such as temperature rise, shrinkage or brittleness.

REFERENCES

- [1] AITCIN P.C., NEVILLE A., "High-Performance Concrete Demystified", *Concrete International*, Vol.15, No.1, pp.21-26, January, 1993.
- [2] GJØRV O.E., "High Strength Concrete", CANMET/ACI Conference on Advances in Concrete Technology, Athens, May, 1992.
- [3] ROY D.M., SCHEETZ B.E., SILSBEE M.R., "Processing of Optimized Cements and Concretes Via Particle Packing", *MRS Bulletin*, pp.45-49, March, 1993.
- [4] OHAMA, 2nd International CANMET/ACI Conference on Fly Ash, Silica Fume, Slag and Natural Pozzolans in Concrete, Madrid, 1986.
- [5] LEWIS J.A., KRIVEN W.M., "Microstructure-Property Relationships in Macro-Defect-Free Cement", *MRS Bulletin*, pp.72-77, March, 1993.
- [6] BACHE H.H., "Densified Cement/ultrafine Particle-Based Materials", Second International Conference on Superplasticizers in Concrete, Ottawa, June, 1981.
- [7] KOKKILA A., "Interaction of Aggregate and Cement Paste in High-Strength Concrete", RILEM 43rd General Council, VTT Symposium 105, August, 1989.
- [8] MOONEY M., "The Viscosity of Concentrated Suspensions of Spherical Particles", *Journal of Colloids*, Vol.6, p.162, 1951.
- [9] STOVALL T., DE LARRARD F., BUIL M., "Linear Packing Density Model of Grain Mixtures", *Powder Technology*, Vol.48, N°1, September, 1986.
- [10] DE LARRARD F., "A General Model for the Prediction of Voids Content in High-Performance Concrete Mix-Design", *Congrès ACI/CANMET Advances in Concrete Technology*, Athènes, May, 1992.
- [11] DE LARRARD F., "Ultrafine particles for the making of very high-strength concretes", *Cement & Concrete Research*, Vol.19, pp.161-172, January-February, 1989.
- [12] CUMBERLAND D.J., CRAWFORD R.J., "The Packing of Particles", Elsevier, 1987.
- [13] FERET R., "Compacité des mortiers hydrauliques (Compactness of hydraulic mortars)", *Annales des Ponts et Chaussées*, 1894.
- [14] DE LARRARD F., "Formulation et propriétés des bétons à très hautes performances (Mix-design and properties of very-high performance concrete)", Doctoral Thesis of Ecole Nationale des Ponts et Chaussées, Rapport de Recherche des LPC N°149, March, 1988.
- [15] DE LARRARD F., LE ROY R., "The Influence of Mix-Composition on the Mechanical Properties of Silica-Fume High-Performance Concrete", 3rd International CANMET-ACI Conference on Fly Ash, Silica Fume, Slag and Natural Pozzolans in Concrete, ACI SP 132-52, Istanbul, May, 1992.
- [16] DE LARRARD F., TONDAT P., "Sur la contribution de la topologie du squelette granulaire à la résistance en compression du béton" (On the contribution of the topology of the aggregate skeleton to the compressive strength of concrete), accepted for publication in *Materials and Structure*, RILEM, October, 1992.
- [17] STOCK A.F., HANNANT D.J., WILLIAMS R.I.T., "The Effect of Aggregate Concentration upon the Strength and Modulus of Elasticity of Concrete", *Magazine of Concrete Research*, Vol.31, No. 109, pp. 225-234, December, 1979.
- [18] DE LARRARD F., "A Method for Proportioning High-Strength Concrete Mixture", *Cement, Concrete and Aggregates*, ASTM, Vol.12, N°1, Summer, 1990.
- [19] HANNA E., LUKE K., PERRATON D., AITCIN P.C., "Rheological Behavior of Portland Cement in the Presence of a Superplasticizer", Third International Conference on Superplasticizers and Other

Chemical Admixtures, Ottawa, ACI SP 119, october 1989.

[20] DE LARRARD F., GORSE J.F., PUCH C., "Comparative Study of Various Silica Fumes as Additives in High-Performance Cementitious Materials", Materials et Structures, RILEM, Vol.25, pp.265-272, 1992.

[21] RICHARD P., CHEREZY M., DUGAT J., "Mortiers à très hautes performances, bétons obtenus à partir de ce mortier et les éléments fabriqués avec ce mortier ou ce béton", INPI, Demande de brevet d'invention, No. 2 677 640, 1992.

LIST OF SYMBOLS

c : packing density of a granular mix

d : smallest size of grains of a granular mix

D : highest size of grains of a granular mix

e_M : Maximum Paste Thickness

$f(z)$: loosening function, depending on the ratio between the sizes of two grain classes

g : aggregate content (in volume)

g^* : packing density of the aggregate

$g(z)$: wall effect function, depending on the ratio between the sizes of two grain classes

$p_1(t)$: cumulated distribution of silica fume (coarsest part)

$p_2(t)$: cumulated distribution of silica fume (finest part)

S_{BET} : specific area of silica fume, measured by the BET method

$y(t)$: voluminal distribution of a granular mix

$\alpha(t)$: specific packing density function, depending on the size of grains t

$\beta(t)$: virtual packing density function, corresponding to a non-random high-density packing

Φ : solid content of a suspension

ρ : density of the silica fume

η_r : relative viscosity of a suspension

$\eta_{r\text{ref}}$: viscosity of a random packing of particles